APPLICATION OF ARC ELASTICITY ANALYSIS METHOD COMBINED WITH CO_2 STORAGE TECHNOLOGY IN BUILDING LOAD AND ENERGY SAVING RETROFIT

by

Liju GAO, Yan ZHOU, Feiyue CHENG, Shile SHI, Yuan WANG, Riliang ZHANG, and Xiaodong WANG**

China Construction Third Bureau Green Industry Investment Co., Ltd., Wuhan, China

Original scientific paper
https://doi.org/10.2298/TSCI2403745G

Analyzing building loads and energy-efficient retrofits is crucial for effective energy management and sustainable development. Strengthening the identification and analysis of factors that impact energy consumption is informative for devising appropriate measures. In order to address the current limitations in analyzing building energy consumption, the present study proposes a combination of the arc elasticity analysis method with CO_2 storage technology. By introducing sensitivity and arc mean elasticity indices, the cooling and heating loads of building energy consumption can be analyzed. Subsequently, a CO_2 refrigeration system and compression process can be designed to optimize the storage of CO_2 and facilitate its role in energy conservation and reduction of energy consumption. Thus, the research aims to fulfill the potential of CO_2 in promoting energy efficiency and reducing consumption. The study utilized software simulation and experimental analysis to examine the impact of the proposed method. The findings revealed a positive correlation between the heat transfer coefficient and the building's annual heat load. In addition, the maximum data variation of the building's cold load was a mere 0.05 per cent, and the relative discrepancy between the software simulation and the actual load values was less than 10 per cent. The exterior building's total cold load value showed a difference of more than 25 per cent when cooled with CO_2 intervention compared to the non-intervention result. Furthermore, the building's maximum load reduction reached 3.4 per cent when uniformly varying the thickness of the insulation layer from 40 mm to 100 mm. The proposed method demonstrates a positive impact on building energy sensitivity analysis. Its energy loss design for various parts of the building could offer useful references for practical engineering designs.

Key words: *arc elasticity analysis, CO_2, building load, energy efficiency technology, sensitivity theory*

Introduction

Energy is essential for enhancing a country's strength, improving quality of life, and promoting economic development. However, overuse of energy is associated with significant environmental and social problems. To address this situation, improving energy efficiency has become an important focus for all industries [1]. One of the goals outlined in the *13th Five-Year*

*Corresponding author, e-mail: xiaodongwang2203@163.com

Plan is to meet energy-saving standards in the construction industry. The plan aims to promote the implementation of energy-efficient technology (EET) in various sectors, including construction and industry, within the framework of resource efficiency. This is a demand that resonates with the public and the country at large [2]. The expansion of building space and the widespread use of heating equipment have increased residents' comfort but also heightened the risk of energy waste. Traditional heating equipment is susceptible to internal and external interference factors, resulting in a fifth of energy loss, with uneven heating being a significant contributing factor [3]. The focus of building EET research is shifting from single energy-saving preservation towards sustained efficiency. An analysis of the degree of sensitivity of building energy efficiency factors to energy consumption can aid in distinguishing between primary and secondary energy efficiency implementation. Sensitivity analysis is a method utilized to evaluate how a model or system is responsive to alterations in input parameters. This analytical approach enables us to comprehend the model's steadiness and resilience. By noting changes in input parameters, examining regular variations is advantageous for decision-making and risk evaluation [4]. Arc elasticity analysis (AEA), a fundamental principle of mechanical equations and materials mechanics, is employed in building load (BL) and energy-saving analysis. This enables assessment of a building's energy consumption and thermal environment to aid in the selection and optimization of measures to save energy [5]. A parameter sensitivity analysis can assist in elucidating the interrelationship between the energy consumption load of a building and its structural parameters. The building arc averaging method enables the analysis of the sensitivity between building energy consumption load and energy-saving renovation technology. It also permits the comparison of the effects of different parameters on building energy consumption load. Furthermore, it provides parameter suggestions and guidance for reducing building energy consumption load in severely cold areas. A sensitivity analysis is a quantitative analysis that examines the degree of influence of a specific factor or a combination of factors on a target variable. A sensitivity analysis of building energy consumption load is a local sensitivity analysis, which is defined as an analysis that examines the impact of single parameter changes on load. In contrast to global sensitivity analysis, arc mean elasticity, as a dimensionless indicator, permits the direct analysis of the sensitivity of different factors to the dependent variable, as well as the analysis of all data pertaining to the target result. The calculation is straightforward and impartial, enabling the ranking of sensitivity between different parameter factors, the analysis of the trend of sensitivity changes of parameters, and the provision of more comprehensive analysis functions [6, 7]. The arc mean elasticity calculation method can be employed to analyze the influence of disparate factors on the annual cooling and heating loads of buildings, circumventing the potential for quantification errors associated with different factors. Furthermore, it enables a comprehensive analysis of BL. Therefore, this study integrates AEA with CO_2 storage technology to enhance building energy efficiency and examines the factors that impact building energy consumption. The ultimate goal is to provide more precise and targeted recommendations. The study innovatively combines AEA and CO_2 technology to analyze building energy efficiency and incorporates a sensitivity analysis to examine the factors that must be considered for retrofitting building energy efficiency, both vertically and horizontally. The ultimate aim is to reduce heating energy costs and wastage whilst ensuring occupants' comfort. The study examines the use of building envelopes and energy conservation by reviewing literature and discussing current EET. The second part of the study focuses on the use of AEA and CO_2 storage technology to address building envelopes and energy conservation. The effectiveness of the methodology is evaluated in the third part of the study using software simulation and case studies. The conclusion summarizes the findings of the full study.

Related works

The distribution of clean energy within China's residential buildings demonstrates notable climatic and geographical features. Scholars Wu [8] analyzed the production and consumption of clean energy using the STIRPAT model and found that solar power and wind energy are the predominant methods of utilizing clean energy in both the northern and southern regions. These results provided valuable data support for the energy upgrade of the city's residential buildings. Guo *et al*. [9] argued that in the current energy-saving retrofit market for existing buildings, energy-saving service companies can better facilitate energy savings by enhancing operational and developmental optimization of the retrofit market. In response to the current severe climate crisis, one of the shallow ground source heat pump systems has demonstrated a broader carbon reduction application with the help of load-bearing structural elements for heat transfer. However, the energy pile analysis in this system technology does not take into account the variability of the spatial medium and is affected by model uncertainty. Based on this, Shi and Wang [10] scholars carried out thermal-mechanical load transfer mechanism analysis and soil parameter modelling with the help of stochastic finite difference model and Bayesian compression perception. The results showed that the method can achieve the quantification of uncertainty index, and it shows good sensitivity to the measurement of structural data. Zhu *et al*. [11] scholars verified with the help of experiments that the insulated concrete wall system exhibits lower energy consumption on the exterior walls of the house, and its thermal mass wall achieves better heat storage. Green roofs can play a better role in thermal insulation, and Cai *et al*. [12] scholars conducted a study on the ecological benefits of green roofs with the help of experimental research and numerical simulation. The results indicated that the design of green roof can effectively play the energy saving and ecological benefits, and the annual carbon emission reduction reached 9.34 kg/m^2, effectively reducing the energy consumption of the building.

Aiming at the current situation and development trend of energy consumption, Li [13] scholars proposed that coal development can be innovated in the directions of development, conversion, carbon capture, utilization and storage, and put forward corresponding key technology descriptions. Li *et al*. [14] established a decoupling effort model between CO_2 and regional economy with the help of two-stage decomposition model and decoupling index, and with the help of data analysis, the researchers believed that accelerating the adjustment of power generation structure can promote the development of power industry. Garimella *et al*. [15] scholars considered the phase-out of synthetic refrigerants used for vapor compression heating as the main current difficulty in the energy section of buildings, based on which he proposed building energy reduction with the help of carbon-free heat and desiccant-coated heat exchanger technology and provided an engineering solution. The results showed that this energy saving method was effective in reducing energy losses and carbon emissions. Liu *et al*. [16] scholars proposed PV, energy storage and flexible building power system operation scheme and constructed a numerical model of PV energy storage with the optimization objective of comprehensive building efficiency. The results demonstrated that the method can effectively control the cost and show better efficiency and effectiveness in energy consumption and carbon emission limitation. For the current oilfield CO_2 capture and storage technology, Guofeng [17] scholars developed a low-energy decarbonization technology based on a new type of activator through simulation calculations and experimental practice, and designed different pipeline network delivery operation modes as well as three kinds of CO_2 recycling and injection technologies. The results showed that this CO_2 sequestration and safety detection technology can effectively achieve low-energy CO_2 capture with good sequestration effect.

Most scholars in the field of building energy efficiency agree that employing clean energy, incorporating insulation materials, designing carbon-free technology, and conducting analysis and design using the STIRPAT model and other numerical models and parameters are beneficial. However, the research undertaken in this area is relatively common and to some extent, it is challenging to analyze the demand for building energy consumption. Therefore, the study integrates both AEA and CO_2 storage technology into structural theory. It examines building energy consumption through software simulation, experimental analysis, process design, and other methods, with the aim of offering practical recommendations for energy efficiency and emission reduction in building design.

Design of AEA combined CO_2 storage technology in building retrofits

The significance of enhancing building energy efficiency as a policy measure for promoting sustainable development is increasingly gaining attention. Given the present state of building energy efficiency and its attendant challenges, this study suggests that a combination of AEA and CO_2 storage technology could be implemented for BL and retrofit analysis. The AEA would examine the building's energy load, while CO_2 storage technology would aid in better energy management and consumption reduction through process design and other means. This combination would support the development of a skills programme and guarantee the practicability of its implementation. The combination of these two factors promotes the creation of targeted skills programmes and guarantees their practicality. Using the arc-elastic mean method to analyze BL and CO_2 technology compression preparation technology, this study focuses on energy saving and consumption reduction. The study analyzes the factors and contents that affect energy demand of buildings, including sensitivity index, compression refrigeration system and compression process. The goal is to provide actionable suggestions for energy-saving renovations and achieve sustainable energy management for buildings.

The AEA design in building load

The AEA in the field of construction engineering is a method of analyzing and evaluating structures, which is used as an analytical method in structural mechanics to analyze the behavior and response of a structure when subjected to forces with the help of the theory of arc elasticity. The method predicts the deformation and stress distribution of a structure under force by considering the arc characteristics of the structure and the elastic properties of the material, which is modeled and analyzed as an approximate numerical method. Analyzing the load response of a building under different environmental conditions can identify energy wastage in the building, and AEA enables the energy flow of a building to be quantified, improving the safety and stability of building analysis [18, 19]. Arc elasticity emphasizes the difference in mean values before and after the change of different demand points on the arc, therefore the study applies the AEA method to the building analysis to design the retrofit from the income of sensitivity analysis of energy consumption factors. Sensitivity analysis theory is originally applied to the theory of the role of incentives in automatic control and economics, which is mainly with the help of quantitative ways to analyze the impact of changes in factors on the target structure, according to the difference in the number of its factors, it can be divided into local sensitivity and global sensitivity analysis. The sensitivity equation can be expressed as:

$$IC = \frac{\partial OP}{\partial IP} = \frac{\Delta OP}{\Delta IP} \tag{1}$$

where ΔOP is the amount of input parameter changes and ΔIP – the amount of output parameter changes. The study is based on the specificity of the research object, and the arc-mean elasticity is chosen as the analysis index, then the equation is changed into:

$$MAE = \left(\frac{\Delta OP}{\Delta IP}\right) \div \left(\frac{\overline{OP}}{\overline{IP}}\right) \tag{2}$$

where $\overline{IP}, \overline{OP}$ is the mean value of input parameters and output parameters in the range of changes. Arc-mean elasticity in the conduct of indicator analysis can directly achieve the degree of sensitivity of different factors change on the dependent variable, and more according to the trend of its change and the interval to determine the degree of sensitivity, has a better objectivity [20]. In the process of BL analysis, the arc-mean elasticity indexes can be introduced in the building cold load, heat load, average cold load, and average heat load to carry out the sensitivity analysis of factor changes. Where the arc-mean elasticity index of cold load can be expressed with the help of:

$$MAE_{AC} = \left(\frac{\Delta OP}{\Delta IP}\right) \div \left(\frac{\overline{OP}}{\overline{IP}}\right) = \left(\frac{\Delta Q_{xc,(x+1)c}}{\Delta a_{x,x+1}}\right) \div \left(\frac{\overline{Q_{xc}}}{\overline{a}}\right), \quad \overline{Q_{xc}} = \frac{\sum_{x=1}^{x=n} Q_{xc}}{n}$$
$$\overline{a} = \frac{\sum_{x=1}^{x=n} a_x}{n}, \quad \overline{MAE_{AC}} = \frac{\sum_{x=1}^{x=n-1} (MAE_{AC})}{n-1} \tag{3}$$

where $\overline{a}$ is the average value, $\overline{Q_{xc}}$ – the average value of a factor over all taken values of building cooling loads, $\Delta a_{x,x+1}$ – the amount of change, $\Delta Q_{xc,(x+1)c}$ – the amount of change in building cooling loads, and $\overline{MAE_{AC}}$ – the average arc-mean elasticity index of building heat loads. The heat load and the associated mean values can be solved similarly along the lines of equation. The average arc-mean elasticity index under different loads can be used to make a horizontal comparison of factors, which in turn affects the sensitivity ranking of the BL impact factor, and can better solve the problem of prioritization in building energy efficiency.

Building energy efficiency involves a wide range and variety of more, and to a certain extent, showing regional and targeted, so the study of building energy efficiency analysis, from the building envelope, building environment heat disturbance control and air conditioning energy saving three aspects of the analysis. The building envelope, including external walls,

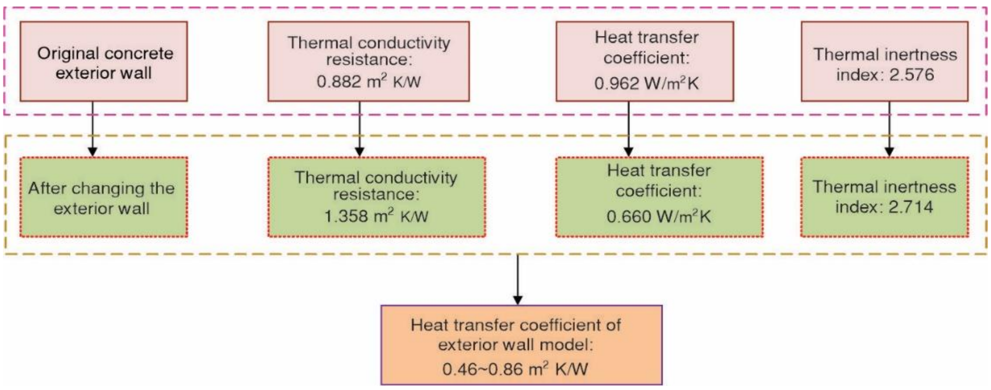

Figure 1. Schematic diagram of sensitivity analysis scheme for external and internal walls of the enclosure structure

external windows, roofs, *etc*., is an important part of energy consumption control, and its loss can basically account for about 60% of the total loss, and different materials and operating methods can lead to changes in heat transfer coefficients in different buildings, and therefore the main EET used are also different [21]. In contrast, the thermal disturbance control of the built environment includes three main aspects: indoor personnel, equipment, and lighting. The study is analyzed in the energy efficiency retrofit of the building based on the limit values of its different structures. Among them, in the external envelope, the study is based on the original wall structure, affecting the heat transfer coefficient by changing the thermal insulation layer, and changing its thickness to achieve load sensitivity analysis. The retrofit programme is shown in fig. 1.

The study is carried out by setting different thicknesses of insulation under the original building envelope coefficients and analyzing the coefficients by varying the difference of the coefficients uniformly for better analysis of the change in cooling and heating loads of the building. The sensitivity of the roof can be analyzed with the help of the same analytical idea, the scheme of which is shown in fig. 2.

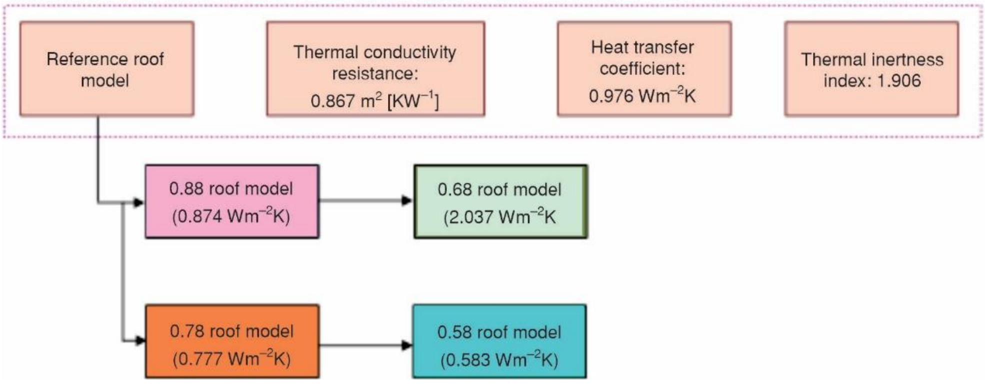

Figure 2. Schematic diagram of roof sensitivity analysis scheme in the enclosure structure

The thickness of the insulation layer can be increased to enhance its thermal insulation performance. However, to achieve energy efficiency benefits simultaneously, a study is conducted to determine the economic thickness using the life cycle depletion method. The mathematical expression of this method is presented in:

$$\delta_{op} = 293.94\sqrt{\frac{PWFC_f DD \cdot \lambda}{H_c C_i \eta}} - \lambda(R_i + R_o + R_w) \tag{4}$$

where δ_{op} [mm] denotes thickness of economic insulation, *PWF* – the discount factor, C_f, and H_c – the coal price and heat generation, *DD* – the number of heating degree days, λ – the thermal conductivity coefficient, C_i – the price of insulation materials, η – the efficiency of the heating system, and R_i, R_o, R_w are the thermal resistance within the wall, outside, and in the envelope, respectively, [22]. The buildings selected by the research institute are situated in cold regions, and their cooling load can be studied using the average value, obviating the necessity for a separate explanation of the cooling load. Nevertheless, the heat load in cold regions is subject to a number of variables. The calculation of the thickness of the insulation layer not only enhances the insulation performance of buildings but also facilitates the observation of energy-saving benefits. Subsequently for the thermal control of the building environment in the sensitivity analysis, such as in the analysis of public buildings need to be analyzed from the personnel density, lighting power two aspects of the analysis, the personnel density and the size of the lighting power will have an impact on the building's energy saving situation.

In the process of building operation, the cooling and heating effect of the air conditioning system will occupy a large proportion of the building energy consumption, common civil building heating design specifications for interior design put forward a certain range of provisions. In the heating condition, the relative humidity is set to be more than or equal to 30% when the temperature is 22~24 °C, at this time, the thermal comfort level is one. Under cooling conditions, the comfort level is one when the temperature and humidity are 24~26 °C and 40~60%, respectively [23]. Therefore, the study needs to calculate the arc-mean elasticity index under different air-conditioning temperatures when carrying out the analysis of the building cooling and heating loads, and select the cooling and heating loads of the space as 2173.49 kW and 1987.54 kW, respectively, with the cooling source being the rated screw chiller and the heating source being the secondary water treated by the plate heat exchanger. At the same time, taking into account the dynamics of the load under the change of outdoor environmental parameters, the pump speed is adjusted with the help of pump frequency conversion technology to reduce the energy consumption of air conditioning. Where the relevant parameters of the water pump change as shown in:

$$\frac{Q_2}{Q_1}=\frac{n_2}{n_1},\ \ \frac{H_2}{H_1}=\left(\frac{n_2}{n_1}\right)^2,\ \ \frac{N_2}{N_1}=\left(\frac{n_2}{n_1}\right)^3 \tag{5}$$

where Q is the flow rate, H – the head, N – the shaft power, and n – the pump speed. Equation (5) references the ratio in the fan water pump, where subscripts 1 and 2 represent water pump machine 1 and water pump machine 2, respectively:

$$\sum_{t=0}^{P_t}(CI-CO)_t=0 \tag{6}$$

where P_t [year] is the static investment payback period, CI [Yuan] – the cash inflow, CO [Yuan] – the cash outflow, and t represents the year. The initial cost encompasses the expenses associated with the construction and subsequent maintenance of the renovated building. The renovation cost encompasses the expense of renovating the outer enclosure structure, which is primarily attributable to the cost of installing the insulation layer. The operating cost primarily affects the cost of maintaining a comfortable internal environment through personnel, lighting adjustments, and air conditioning energy conservation.

The CO_2 storage technology design for building energy retrofits

The CO_2 storage technology is an important method of combating climate change and carbon emissions by safely storing captured CO_2 gas in underground rock reservoirs to reduce CO_2 technology in the atmosphere. Commonly applied CO_2 storage technology is realized with the help of carbon capture and sequestration technology, or CO_2 is used as a building refrigerant or heating medium to perform heat transfer properties, which in turn achieves the effect of reducing energy consumption [24]. Also the application of CO_2 storage technology in materials can better improve the insulation and heating system of buildings, reduce the dependence on traditional energy sources, and reduce the energy consumption of buildings [25]. In order to reduce building energy consumption, the study is based on the principle of CO_2 compression refrigeration, clean CO_2 as a refrigerant for thermal insulation research, the system content includes compression refrigeration system as well as two aspects of the thermal insulation system, its system layout structure diagram shown in fig. 3.

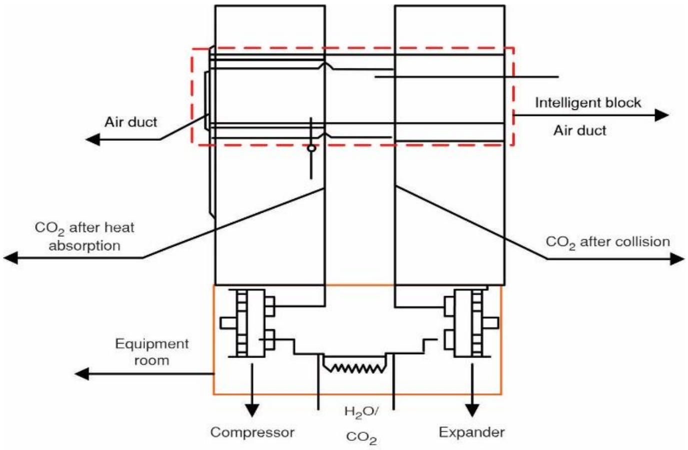

Figure 3. Schematic diagram of CO_2 compression system

While the compression refrigeration system consists of a compressor, a cooler, an expander and a heat exchanger, the insulation system consists mainly of intelligent ducts attached to the building surface. The low temperature, low pressure CO_2 is heated up in the ducts and then compressed adiabatically for specific zones. The CO_2 can enter the heat exchanger in the smart duct for constant pressure heat absorption after processing in the refrigeration system to reduce its surface temperature, forming a cycle between the two systems. In the analysis of the energy consumption of the building, it is analyzed with the help of the thermal time constant model of the building mass, which considers the presentation of a particular temperature as a superposition of several temperature process effects, the mathematical expression of which can be seen in:

$$t_a(\iota) = t_b + \Delta t_{sol}(\iota) - \Delta t_{lw}(\iota) \tag{7}$$

where $t_a(\iota)$ is the air temperature, $t_a(\iota)$ – the base temperature, $\Delta t_{sol}(\iota)$ – the change in air temperature due to solar radiation heat in the building complex, $\Delta t_{lw}(\iota)$ – the falling temperature under long wave radiation, and ι – the calculation time. Changes in solar radiation cause the heat situation in the air to occur waveforms of which the change in temperature due to changes in solar radiation can be expressed as:

$$\Delta t_{sol}(\iota) = \frac{m}{\alpha}\sum_{\lambda=0}^{\lambda=\iota} \Delta I_{pen}(\iota)\left[1 - \exp\left(\frac{\lambda - t}{CTTC}\right)\right] \tag{8}$$

where *m* is the solar radiation absorption rate of the lower mat surface, α – the integrated heat transfer efficiency, $\Delta I_{pen}(\iota)$ – the time-averaged step of daily direct solar radiation illumination per unit area, and *CTTC* – the thermal time constant of the building complex. The heat transfer brought about when solar radiation irradiates the building façade can be calculated as a time-dependent cold load, the mathematical expression of which is given in:

$$Q = K_o F_o\left[\left(t_{lo} - t_{dl}\right)C_a C_p - t_n\right] \tag{9}$$

where K_o is the heat transfer coefficient of the external wall, F_o – the area of the external wall, t_{lo} – the hour-by-hour value of the cold load, t_{dl} – the location correction coefficient of the enclosure, C_a – the corrected value of the exothermic coefficient of the external surface, and C_p – the corrected value of the solar absorption coefficient of the external surface of the enclosure. In the building structure, for the temperature increase of CO_2 in the duct in the calculation model, where the thermal time constant can better reflect the heat storage capacity of the structure. Where the integrated heat transfer coefficient is under the consideration of radiation and convection effects, where the average integrated heat transfer coefficient under the urban cover can be expressed as:

$$\alpha = \varepsilon\alpha_r + \alpha_v \tag{10}$$

where ε is the emissivity of the cryogenic surface, α_r – the radiative heat transfer coefficient, and α_v – the convective heat transfer coefficient caused by the wind speed of the lower mat. The primary function of CO_2 storage technology is to alter the flow rate of gas by compressing its volume. This principle has been the subject of research into the use of clean CO_2 as a refrigerant and insulation. The parameters that influence CO_2 storage technology include the efficiency of the compression machine and the settings of external conditions (air ducts). In the absence of alterations to the volume and coverage area of the exterior wall, the supplementary cooling capacity resulting from solar radiation within the building can be diminished by the installation of air ducts on the surface of the wall. A study is conducted on building models to assess the impact of air ducts on heat transfer. The study considers a CO_2 flow thickness of 20 mm and a thermal conductivity of 0.08 W/m^2°C. The findings are used to modify the formula and derive an:

$$\alpha_c = \frac{1}{\left(\dfrac{1}{\alpha_r} + \dfrac{\delta}{\lambda} + \dfrac{1}{h}\right)} \tag{11}$$

where α_c is the corrected comprehensive heat transfer coefficient, h – the convective heat transfer coefficient of the air duct, λ – the absorption rate of the underlying surface, and δ – the wind speed.

The current carbon capture for CO_2 is still facing high cost and material sustainability issues, the research design analyses the CO_2 compression system to better achieve energy saving and consumption reduction. the CO_2 compression process flow is shown in fig. 4.

The decarbonized CO_2 gas is removed from impurities by a droplet separator, cooled by pressure compression, and the separated oil and water products are fed into the desulphurization process for desulphurization, filtration, compression and cooling until the final product is fed into the high pressure synthesis system. It should be noted that the volume of CO_2 gas decreases more quickly, and in practice, the production load of the compression system is usually related to the gas flow rate value, then with the help of the Klaber equation and the mass of the substance for deduction, when the temperature of the compressed gas rises, it is easy to cause the system of ammonia-carbon ratio imbalance, so it is necessary to pay attention to the system cooling and loading situation.

Effectiveness of the application of combined treatment technology in building load and energy saving retrofits

In the experimental process, the study is carried out with the help of Designers Simulation Tookit (DeST) software for building model construction and analysis, DeST software to

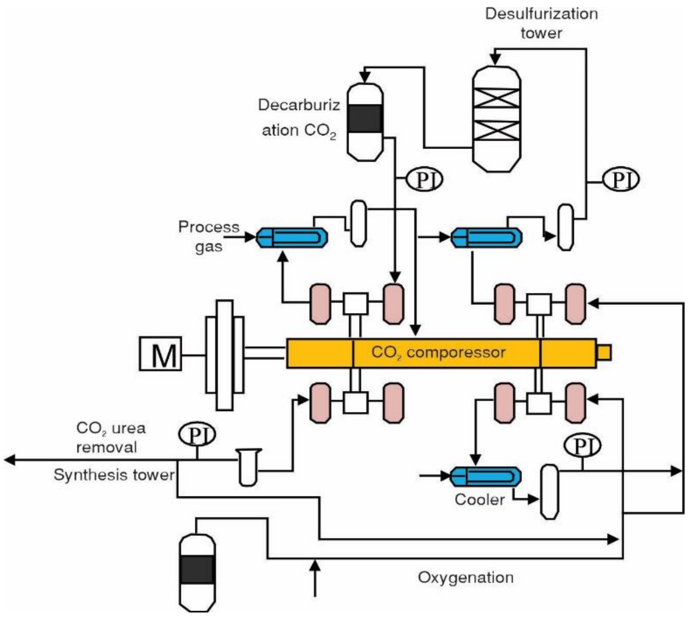

Figure 4. Schematic diagram of CO_2 compression process

natural room temperature for building and environmental control links, its design and simulation process of the stage can better reflect the idea of the stage of the sub-points, and the software also has a good inclusiveness and openness. The DeST software includes indoor lighting module, natural ventilation simulation module, meteorological module, building shading calculation, and air conditioning system scheme and air handling equipment module, *etc*. An old building in a city with a height of 23 m and a floor area of 6500 m^2 is selected as the object of the study, and its floors are divided into an above-ground part (6 floors) and a below-ground part (1 floor). At the same time, the building area has a typical oceanic climate, with an average annual temperature and average precipitation of 12.5 °C and 778 mm, respectively, and the outdoor humidity and solar radiation in the area can be seen in fig. 5.

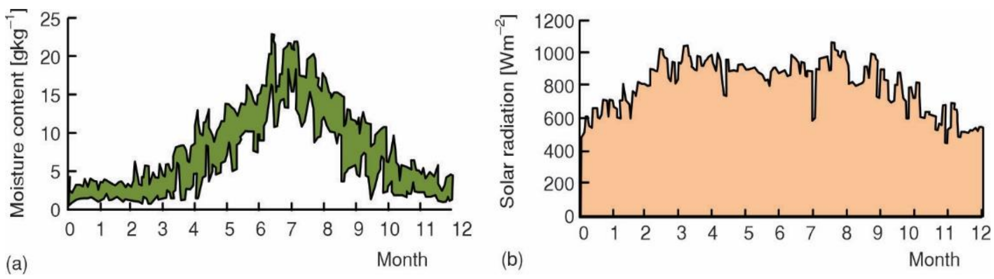

Figure 5. Outdoor moisture content and solar radiation; (a) outdoor moisture content and (b) outdoor solar radiation situation

The maximum humidity of the air in this area can reach 15.51 g/kg, and the maximum solar radiation can reach 1066.05 W/m^2, and the overall data shown has a large fluctuation and seasonality. The objective is to analyze the energy consumption status of the building area, with a particular focus on the above-ground portion. The original building prototype featured curved walls, which the DeSt software is unable to accurately represent. Consequently, the study simplified the curved walls during wall construction and designed them in the form of multiple line segments. During the model construction process, the merging of air-conditioned rooms with the same orientation yields a schematic diagram of the model, as illustrated in fig. 6.

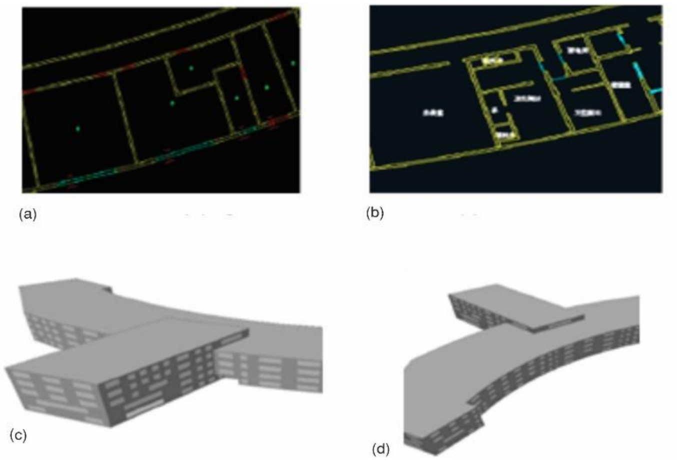

Figure 6. Building model diagram; (a) DeSt model of the building, (b) Architectural prototype diagram, (c) southeast side of the DeSt model of the building, and (d) northeast side of the architectural DeSt model

Subsequently, the parameters of the building model are designed, and the detailed results of its parameters are shown in tab. 1.

Table 1. Parameter information table

Building structure		Structural materials	Structural parameters	Heat transfer coefficient K [Wm^{-2}K^{-1}]
Enclosure structure	Exterior wall	Mixed mortar reinforced concrete polystyrene cement mortar	200 mm insulated wall	0.96
	Inner wall	Cement mortar - reinforced concrete - cement mortar	140 mm thick wall	/
	Floor	Reinforced concrete cement mortar	200 mm thick concrete	1.1
	Floorslab	Cement mortar - reinforced concrete - cement mortar	150 mm reinforced concrete	2.7
	Roof	Oil felt cement mortar polystyrene reinforced concrete mixed mortar	120 mm insulation and waterproof layer	0.98

For the thermal disturbance parameters of the building, the study makes a comprehensive judgement based on the energy saving design standard for public buildings, setting typical room parameters, including the lighting situation, the flow of people and the air-conditioning system settings. It is recommended that load sensors be installed in various key locations of the building, including power, lighting, air conditioning, and heating, in order to monitor energy consumption in real-time and record daily, weekly, or monthly energy consumption data of the building. This data should include electricity consumption, water consumption, and gas consumption, among other things. Additionally, the energy consumption of various parts of the building at different time periods should be monitored, including that of enclosure structures, air conditioning energy efficiency, and so forth. The data obtained from real-time monitoring must be processed, analyzed, and compared in order to ascertain the actual load situation of the building. Subsequently, the cooling and heating load conditions of the building can be simulated and calculated, with the results presented in fig. 7.

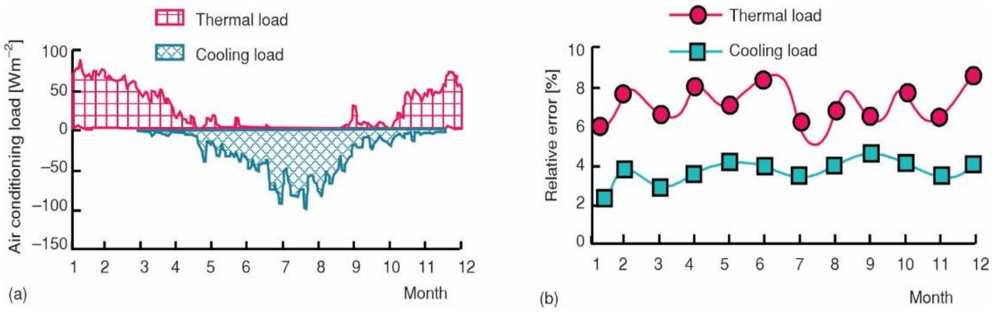

Figure 7. Calculation results of cooling and heating load for buildings; (a) annual hourly air conditioning load per unit area and (b) relative error results between simulated and actual load results

Figure 7 shows that the software simulation results in the load situation and the actual results are generally the same, the maximum cooling load of 1963.25 kW, the maximum heat load of 1828.02 kW. The simulation results and the actual results in the maximum cooling load and the maximum heat load of the relative error results in the maximum load of not more than 10%, the data are 8.64% and 8.23% respectively. The reason for this result is that the simulation software can grasp the relationship between different structural parameters in a dynamic way, and the error exists due to the fact that the actual results are presented as instantaneous results, and the load results will be somewhat different due to the way of calculating the heat transfer

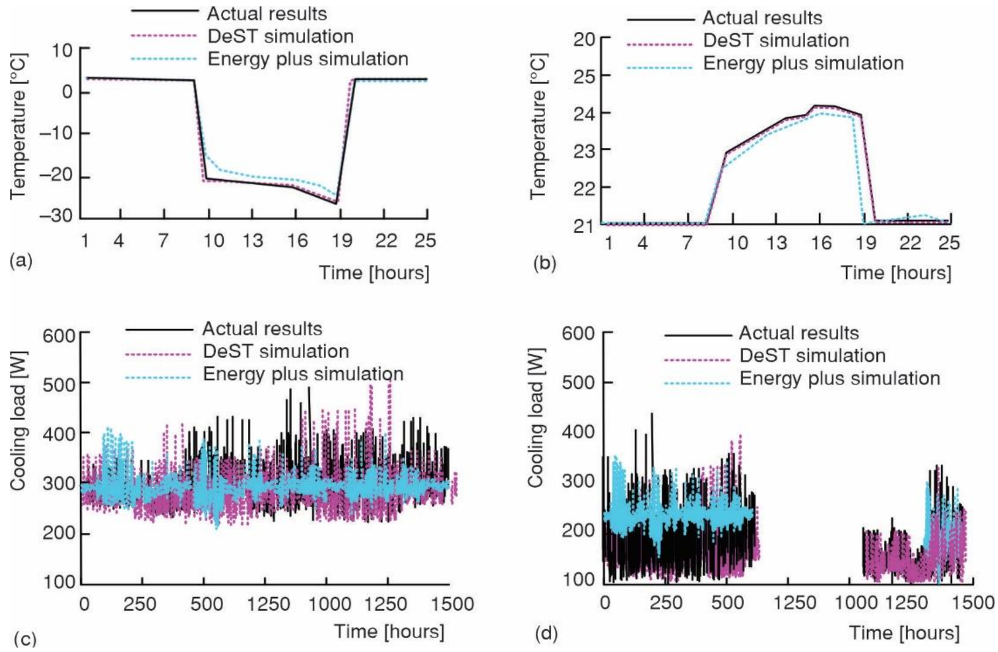

Figure 8. Test results of different simulation software; (a) winter daily room temperature, (b) summer day room temperature, (c) room cooling load and (d) room heat load

coefficient. A comparative analysis is conducted on the simulation models proposed in the study. To facilitate a meaningful comparison, a room in the northwest corner of the building is selected for analysis under identical parameter settings. The results are presented in fig. 8.

Figure 8 illustrates a notable discrepancy between the indoor temperature estimates generated by the two software programs and the actual measurements. In particular, during the summer months, the EnergyPlus simulation software exhibits an average discrepancy of at least 0.5% in comparison to the actual results, which is observed after a period of over 10 hours. Conversely, during the winter season, a certain degree of discrepancy persists between the simulation results of the EnergyPlus software and the actual results. The simulation outcomes of the DsST software proposed in the study are highly concordant with the actual outcomes. Furthermore, the discrepancy between the simulation results of the EnergyPlus software and the actual data in terms of heat and cooling loads exceeds 5%. Additionally, there is a lack of data in the simulation results under heat load conditions. The aforementioned results demonstrate that the simulation software proposed in the study is effective in practice. The study takes into account the economy and rapidity in the process of energy-saving renovation, the study changes the original heat transfer coefficient of the building, and analyses the sensitivity of the building under the arc-elastic mean index, and the results are shown in fig. 9.

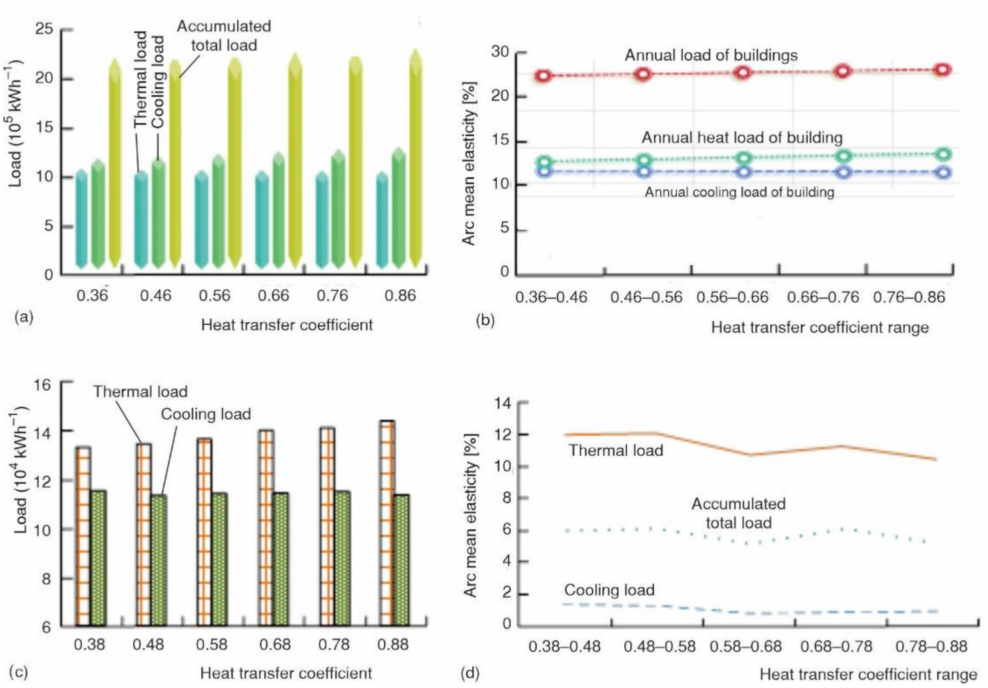

Figure 9. Load situation and arc mean index of exterior walls and roofs

The results in fig. 9 show that there are some differences in the BL situation at different heat transfer coefficients for the exterior walls. Specifically, there is a positive relationship between the heat transfer coefficient and the annual heat load of the building, and at a coefficient of 0.86 W/m^{2}K, reaching a maximum heat load of 143289.11 kWh. The data change of the building cold load is overall smaller, and its effect is much smaller than that of the heat load, with the maximum change in the data reaching 0.05%. From the BL arc-mean elasticity values,

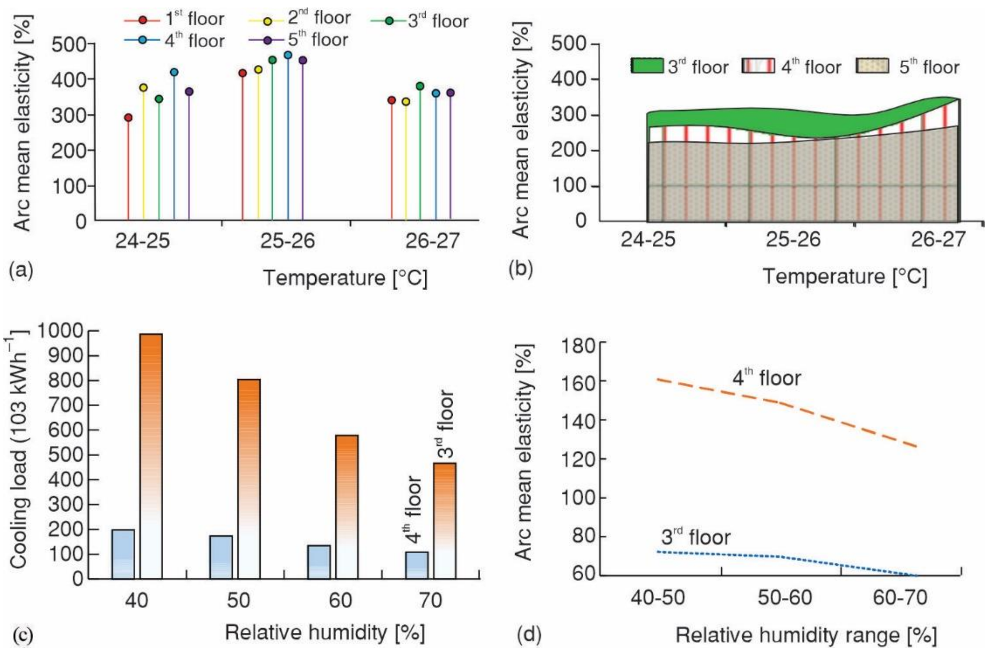

Figure 10. The BL and arc mean under different temperatures and humidity;
(a) changes in cooling load on different floors, (b) heat load changes on different floors,
(c) cooling load of building floors under different humidity levels, and
(d) cooling load of building floors under the same humidity

the maximum values of arc-mean elasticity of cold load and arc-mean elasticity of heat load are 3.08 per cent and 14.13 per cent, and the average arc of the total load is 6.05 per cent for the range of heat transfer coefficients of the external walls from 0.36 W/m^{2}K to 0.86 W/m^{2}K. The overall trend of numerical changes in the three curves is relatively stable, and the building heat load is more sensitive under the change of the number of heat transfers from the external walls. Subsequently, the BL of the air-conditioning system at different temperatures is statistically analyzed, and the results are shown in fig. 10.

Figure 10 results show that when the air-conditioning temperature setting temperature of 25 °C to 26 °C, the arc mean elasticity value of the comprehensive cold load of the building changes basically more than 300 per cent, and with the rise of the building floors, the average value of its cold load also shows slight fluctuations, but fluctuations of no more than 5 per cent, the building's heat load change is slightly lower than the cold load situation. Rooms with higher floors are more sensitive to cold temperature changes than to heat loads. The humidity condition is varied from 40% to 70%, the study selected the rooms of the floors with intermediate number of floors for load sensitivity analysis and the results showed that the reduction of humidity in the rooms brings about a reduction in the cold load. The arc-mean elasticity change curves of the cooling loads of different floor buildings show a decreasing trend, where the 3rd floor has a reduction of 54126.27 kWh when the humidity is reduced from 70% to 40%. Subsequently, the energy effect of the pump regulation method proposed by the study is analyzed and the results are shown in fig. 11.

The results in fig. 11 show that the pump-regulated system shows a reduction in energy consumption compared to the theoretical data, and the reduction in energy consumption

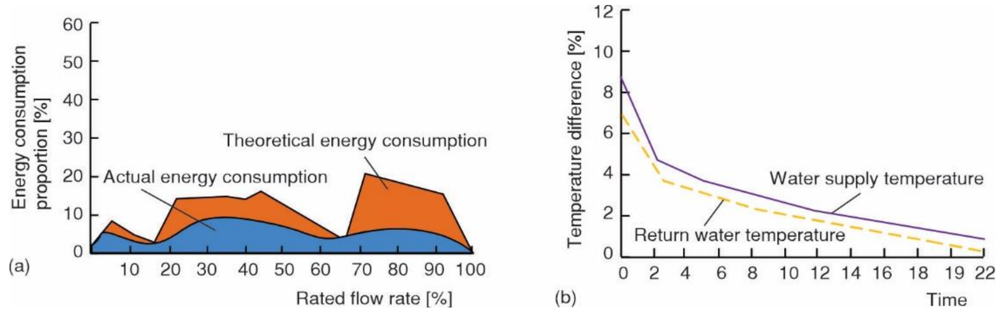

Figure 11. Energy consumption and temperature difference changes under water pump regulation method; (a) water pump energy consumption and (b) temperature difference between supply and return water of air conditioning chilled water

reaches a maximum of 16.54% at a rated flow rate of 70%. The overall trend seems to be that the improved method results in a significant reduction in energy consumption. At the same time, the supply and return water data of the air conditioning system also showed that the temperature difference between the water temperature decreased significantly, with the maximum temperature difference decreasing from 8.5 ℃ to 0.4 ℃. The cooling load of the building with CO_2 technology is then analyzed and the results are shown in fig. 12.

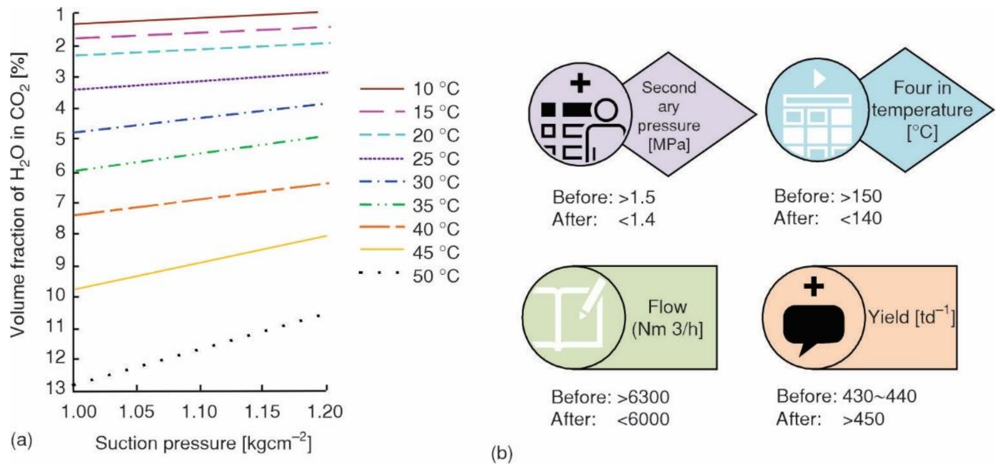

Figure 12. The CO_2 application effect; (a) moisture content of CO_2 under different temperature and pressure and (b) equipment operating parameters before and after application

Figure 12 shows that with the gradual increase of the compressor suction temperature, the water content volume fraction of CO_2 is showing a decreasing trend, which shows an average water volume fraction of 1.4% at a temperature of 10 ℃, and an average water volume fraction of 11.83% at a temperature of 50 ℃. After the application of CO_2 compression technology, the parameters of the equipment also changed, in which the second out pressure, four into the temperature are less than 1.4 MPa and 140 ℃, and the flow rate and output are also improved compared with the application of the former. The above results show that CO_2 compression technology can better reduce the water content in the system, which is helpful for the reduction of energy consumption in the compression process of the system. In addition, the BL situation under CO_2 cooling technology is statistically analyzed and the results are shown in tab. 2.

Table 2. Changes in cooling load of exterior wall buildings under CO_2 cooling intervention

Hourly cooling of external walls [kW]						
Time	3	6	9	12	15	18
Total load without CO_2 [kW]	6.25	6.81	9.68	9.64	11.03	9.89
Total load with CO_2 [kW]	6.22	6.51	8.47	8.53	8.25	8.24
Total cooling load under duct setting [kW]						
Time	3	6	9	12	15	18
Heat transfer	2.06	2.21	1.49	1.39	1.81	2.79
Radiation	1.05	1.18	4.02	3.74	4.46	2.62
Sensible heat	0.76	0.82	1.04	1.06	1.07	1.07
Latent heat	3.03	3.03	3.03	3.03	3.03	3.03

The results in tab. 2 show that the total cooling load values of the facade building under CO_2 intervention cooling are significantly lower than the results without intervention, and the maximum load difference between the two is more than 2 kW with the enhancement of time, with the maximum difference magnitude exceeding 25%. The cold loads on the façade of the building show a small overall fluctuation over time, with the loads changing from 6.22 kW to 8.53 kW in the intervention scenario, with a variation of 37.13%. The heat transfer values of the façade with air ducts reached the minimum (1.49 kW) and maximum (2.79 kW) values at 9 and 18 hours, with a significant improvement in the radiant effect. The CO_2 treatment has a significant intervention effect on the cold load of the building. The total cooling load of the exterior wall after setting up the air duct is statistically analyzed, and the results are shown in tab. 3.

Table 3. Total cooling load of outer wall after air passage setting

Load [J]	4	8	12	16	20
Heat transfer	1.98	1.44	1.16	1.73	2.56
Radiation	0.95	3.47	3.54	4.12	2.42
Sensible heat	0.57	0.79	0.86	0.86	0.86
Latent heat	2.82	2.82	2.82	2.82	2.81

The results presented in tab. 3 demonstrate that following the installation of air ducts, the cooling load changes of the building exhibit a relatively stable pattern over different time periods, with a notable reduction in the value of radiation heat. Further analysis is conducted on the compression system proposed in the study, and the results are presented in fig. 13.

The results presented in fig. 13 demonstrate that the energy consumption of the compressor exhibits a notable decline across a range of heat transfer efficiencies, with a reduction from 80 kW to 68 kW. The energy consumption of the cooler is also affected, with a decrease from 70 kW to 60 kW. The numerical alterations to the heat exchanger are relatively minor. With an increase in heat exchange efficiency, there is a notable decline in the thermal efficiency of the compressor and cooler. Consequently, the operational efficiency can be enhanced by optimizing the heat transfer efficiency of the compressor within the compression system. Subsequently, a technical and economic analysis is conducted on the simulation method proposed in the study. This analysis reveals that the extruded polystyrene insulation performed better in terms of price and cost, as well as economic thickness. Consequently, the results of the BL simulation are analyzed first, and different thicknesses of the insulation are set up. The contents of these simulations are shown in fig. 14.

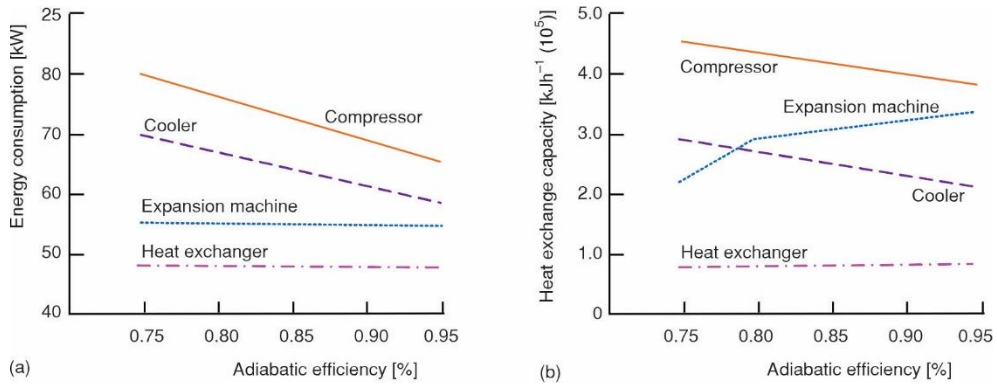

Figure 13. Energy consumption and heat exchange of different components; (a) component energy consumption and (b) component heat exchange

The results presented in fig. 14 demonstrate a linear decrease in the heat load per unit area as the thickness of the external wall insulation increases under the software model simulation. This leads to an external wall heat load of 65.23 kWh/m^2 when the insulation layer reaches a thickness of 100 mm. Furthermore, the area heat load reduction is positively proportional to the energy saving investment. The results of the load reduction rate demonstrate that when the thickness of the insulation layer undergoes a uniform change from 40 mm to 100 mm, the values are 3.4%, 2.2%, 1.7%, 1.4%, 1.2%, 0.7%, 0.6%, and that the energy saving reduction after the thickness exceeds 80 mm is less than 1%. The result is in close alignment with the actual theoretical results, which demonstrate the efficacy of the model simulation analysis. Subsequently, a number of different methods are employed to assess the applicability of insulation materials. The results of these analyses are presented in fig. 15.

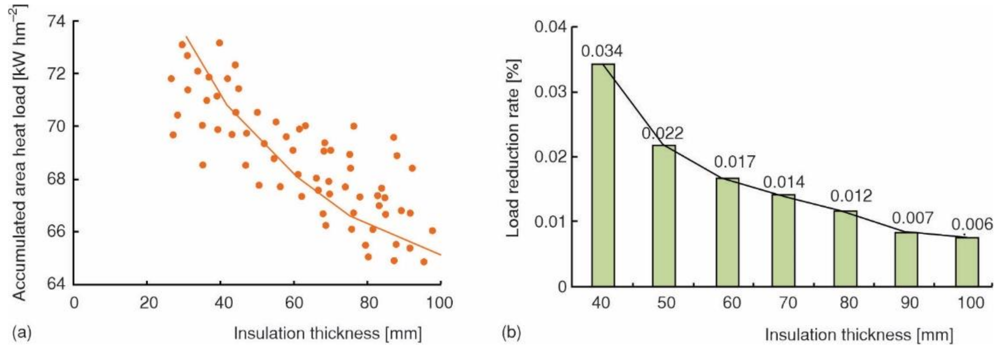

Figure 14. Heat load per unit area and load reduction rate of buildings under different insulation layers; (a) area heat load under different insulation layer thicknesses and (b) load reduction rate under different insulation layer thicknesses

The results in fig. 15 show that the exterior wall and roof insulation have better economic indicators at different initial investment costs, with values above 0.5 and 0.6, and the insulation effectiveness of both is less affected by the experimental cycle time. The above results show that the material selection method proposed by the study can greatly save costs and reduce energy consumption in terms of revenue investment. The data on the recovery benefits and investment cycle time of the insulation materials are also analyzed and the results are shown in fig. 16.

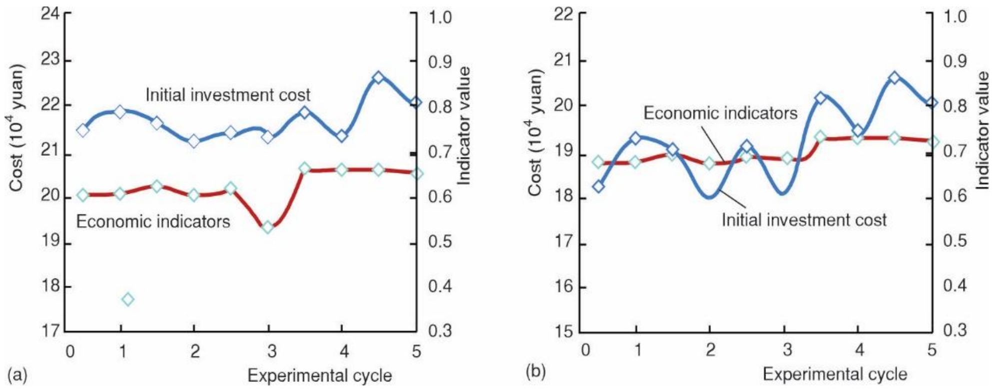

Figure 15. Economy of building structural insulation materials; (a) external wall economy and (b) roof economy

The results in fig. 16 show that the static payback periods for building facades and roofs are shorter, with minimum values of 8.23 and 6.11 years, and that their overall initial investment in insulation effectiveness is relatively smooth, with fluctuations of no more than 7 per cent, which makes them overall more economical.

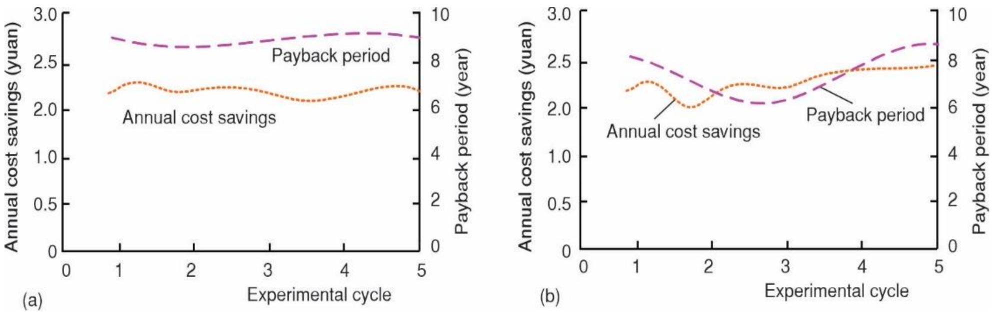

Figure 16. Recyclability of building structural insulation materials; (a) external wall economy and (b) external roof economy

Conclusion

Considering the present state of BL and energy-saving research, the research aims to conduct a combined investigation of AEA and CO_2 storage technology. Furthermore, it chooses a building district in a city for testing and analysis. The study revealed that the software simulation accurately reflected the loading conditions, with relative errors of 8.64% and 8.23%. The maximum cooling load was measured at 1963.25 kW, while the maximum heat load at 1828.02 kW. The analysis of the building's sensitivity to variations in heating and cooling showed a positive correlation between the heat transfer coefficient and the building's heat load throughout the year. The coefficient value was 0.86 W/m^{2}K. This resulted in a maximum heat load of 1432089.11 kWh. The air-conditioning system load results indicated that the fluctuation of the average cold load value did not surpass 5%. Additionally, the cold load mean value's elasticity change curve for different floors of the building illustrated a declining pattern. Following the adjustment of the water pump in the air conditioning unit, the energy consumption decreased to a maximum of 16.54% when operating at 70% of the flow rate. Additionally, improvements were observed in temperature stability. The CO_2 technology outlined in the study indicated average water volume percentages of 1.4% and 11.83% at 10°C and 50°C correspondingly. The façade's heat transferred load values with a duct setup had reached a minimum (1.49 kW) and maximum (2.79 kW) at 9 and 18 hours, respectively, with significant intervention impact. The heat load per unit area of the external wall exhibited a linear decrease, with the heat load amounting to 65.23 kWh/m^2 at an insulation layer thickness of 100 mm. Once the layer thickness surpassed 80 mm, the decrease in energy savings due to insulation became negligible, with a result close to the theoretical standards. The initial investment value in the building under the research procedure did not fluctuate by more than 7%, and the general economy is favorable. Essential future study elements include enhancing the use of new materials in the CO_2 compression process and analyzing various index factors that influence the building economy.

Data availability

The datasets used and/or analyzed during the current study available from the corresponding author on reasonable request.

References

[1] Yang, X., *et al.*, Energy-Saving Potential Prediction Models for Large-Scale Building: A State-of-the-Art Review, *Renew. Sust. Energ. Rev., 156* (2022), Mar., pp. 111992.1-111992.14
[2] Donglin, D. Z., *et al.*, Research on Large-Scale Building Energy Efficiency Retrofit Based on Energy Consumption Investigation and Energy-Saving Potential Analysis, *J. Energ. Eng.-ASCE, 145* (2019), 6, pp. 04019024.1-04019024.14
[3] Xue, P., *et al.*, Optimization of Window-to-Wall Ratio with Sunshades in China Low Latitude Region Considering Daylighting and Energy Saving Requirements, *Appl. Energ., 233/234* (2019), Jan., pp. 62-70
[4] Carpineti, M., *et al.*, Embedding Physics Into Technology: Infrared Thermography and Building Inspection as a Teaching Tool — A New Participated Strategy Approach to the Physics of Heat Transfer and Energy Saving for Professional Schools, *Can. J. Phys., 97* (2019), 9, pp. 1019-1026
[5] Chi, F., *et al.*, Integration of Radiative-Based Air Temperature Regulating System Into Residential Building for Energy Saving, *Appl. Energ., 301* (2021), 2, pp. 117426.1-117426.17
[6] Tang, Z., *et al.*, Sensitivity and Reliability Analysis Method of Interval Uncertainty Parameters, *CIMS., 23* (2017), 12, pp. 2593-2603
[7] Huynh, A., *et al.*, Energy-Efficiency Requirements for Residential Building Envelopes in Cold-Climate Regions, *Atmosphere., 12* (2021), 3, 405
[8] Wu, L. W., Clean-Energy Utilization Technology in the Transformation of Existing Urban Residences in China, *Int. J. Coal Sci. Technol., 8* (2021), 5, pp. 1138-1148
[9] Guo, H.-D., *et al.*, Optimization and Implementation Strategy of ESCO Driving Force in the Development of Energy-Saving Transformation Market of Existing Buildings, *Ecological Economy, 17* (2021), 4, pp. 301-314
[10] Shi, C., Wang, Y., Stochastic Analysis of Load-Transfer Mechanism of Energy Piles by Random Finite Difference Model, *J. Rock Mech. Geotech., 15* (2023), 4, pp. 997-1010
[11] Zhu, L., *et al.*, Detailed Energy Saving Performance Analyses on Thermal Mass Walls Demonstrated in a Zero Energy House, *Energy Build., 41* (2009), 3, pp. 303-310
[12] Cai, L., *et al.*, Reduction in Carbon Dioxide Emission and Energy Savings Obtained by Using a Green Roof, *Aerosol Air Qual. Res., 19* (2019), 11, pp. 2432-2445
[13] Li, Q., The View of Technological Innovation in Coal Industry Under the Vision of Carbon Neutralization, *Int. J. Coal Sci. Technol., 8* (2021), 6, pp. 1197-1207
[14] Li, R., *et al.*, A Region-Scale Decoupling Effort Analysis of Carbon Dioxide Emissions From the Perspective of Electric Power Industry: A Case Study of China, *Environ. Dev. Sustain., 25* (2023), 5, pp. 4007-4032

[15] Garimella, S., *et al.*, Realistic Pathways to Decarbonization of Building Energy Systems, *Joule, 6* (2022), 5, pp. 956-971
[16] Liu, C., *et al.*, Energy Management and Capacity Optimization of Photovoltaic, Energy Storage System, Flexible Building Power System Considering Combined Benefit, *Energy Eng., 120* (2023), 2, pp. 541-559
[17] Guofeng, W., Carbon Dioxide Capture, Enhanced-Oil Recovery and Storage Technology and Engineering Practice in Jilin Oilfield, NE China, *Petrol. Explor. Dev.+, 50* (2023), 1, pp. 245-254
[18] Mehrjerdi, H., *et al.*, Unified Energy Management and Load Control in a Building Equipped with Wind-Solar-Battery Incorporating Electric and Hydrogen Vehicles Under Both Connected to the Grid and Islanding Modes, *Energy, 168* (2019), 1, pp. 919-930
[19] Alam, M., *et al.*, Energy Saving Performance Assessment and Lessons Learned From the Operation of an Active Phase Change Materials System in a Multi-Storey Building in Melbourne, *Appl. Energ., 238* (2019), 15, pp. 1582-1595
[20] Ulpiani, G., *et al.*, On the Cooling Potential of Elastocaloric Devices for Building Ventilation, *Sol. Energy, 230* (2021), Dec., pp. 298-311
[21] Zeinal-Kheiri, S., *et al.*, Real-Time Energy Management in a Microgrid with Renewable Generation, Energy Storages, Flexible Loads and Combined Heat and Power Units Using Lyapunov Optimization, *IET Renew. Power Gen., 14* (2020), 4, pp. 526-538
[22] Liu, X., *et al.*, Optimization of Insulation Thickness of External Walls of Residential Buildings in Hot Summer and Cold Winter Zone of China, *Sustainability., 12* (2020), 4, 1574
[23] Terlouw, T., *et al.*, Life Cycle Assessment of Direct Air Carbon Capture and Storage with Low-Carbon Energy Sources, *Environ. Sci. Technol., 55* (2021), 16, pp. 11397-11411
[24] Idris, A. M., *et al.*, Energy Conversion and Conservation Technology in Facing Net Zero-Emission Conditions and Supporting National Defense, *Trends Renewable Energy, 8* (2022), 1, pp. 49-66
[25] Usman, A. M., Abdullah, M. K., An Assessment of Building Energy Consumption Characteristics Using Analytical Energy and Carbon Footprint Assessment Model, *Green Low-Carbon Economy, 1* (2023), 1, pp. 28-40

Paper submitted: January 12, 2024
Paper revised: March 15, 2024
Paper accepted: April 29, 2024